View Article Online
View Journal

ChemComm
Chemical Communications

Accepted Manuscript

This article can be cited before page numbers have been issued, to do this please use: Y. Tsuchiya, R. Onai, D. Uraguchi and T. Ooi, *Chem. Commun.*, 2020, DOI: 10.1039/D0CC04821F.

ROYAL SOCIETY OF CHEMISTRY

rsc.li/chemcomm

View Article Online
DOI: 10.1039/D0CC04821F

COMMUNICATION

Redox-Regulated Divergence in Photocatalytic Addition of α-Nitro Alkyl Radicals to Styrenes

Yuto Tsuchiya, Ryota Onai, Daisuke Uraguchi, and Takashi Ooi*

Received 00th January 20xx,
Accepted 00th January 20xx

DOI: 10.1039/x0xx00000x

A divergent photocatalytic system for the reaction of α-bromo nitroalkanes with styrene derivatives is established, wherein the generation of the persistent nitroxyl radical as a junctional intermediate and proper tuning of the redox ability of the system constitute the crucial elements for achieving regorous control over the possible reaction pathways.

Divergent synthesis is a combination of protocols for independently producing two or more products from an identical set of starting materials, providing a powerful means for constructing a library of synthetic building blocks. Various divergent systems have been developed for two-electron, ionic reaction manifolds by choosing proper catalysts and adjusting reaction conditions. The reaction pathway to each product is determined by the energetic discrimination of the transition states of the possible competing pathways.[1] On the other hand, efforts toward developing single-electron-mediated variants of divergent reactions have met with limited success, partially due to the difficulty in discriminating the energy level of the respective transition state in the radical processes. In this regard, recent significant progress in photoredox catalysis research offers a unique opportunity to develop divergent radical reactions.[2-8] For instance, upon considering the general mechanism of a redox-neutral photoredox reaction, a photocatalyst (PC) undergoes both single-electron oxidation and reduction with substrates and intermediates during a single catalytic cycle, where the timing and order of the redox events are critically important in dictating the reaction pathway for the selective formation of a single product (Fig. 1a). In a typical case conceivable for a divergent photoredox system, an initial redox event with a PC under light irradiation triggers the bond formation between substrates to generate a radical intermediate. From this junctional intermediate, the sequence of the second redox event and the product-determining bond formation causes divergence in the product structure. Accordingly, the reaction pathway primarily depends on the difference in the redox potentials of the junctional intermediate and the PC (PC A or PC B), which is inherently different from what determines the pathway in common ionic divergent reactions. Despite their distinct features and synthetic potential, however, the redox-regulated, divergent radical reactions remain scarce[2] and are largely restricted to substrate-controlled systems.[6,7] Here, we report a rigorously divergent product formation in the addition of α-nitro alkyl radicals to styrenes enabled by tuning the redox ability of the photocatalytic system.

Our approach arose from the understanding that the underlying problem associated with the development of catalyst-directed, divergent photoredox reactions would be the low concentration of the short-lived radical intermediate generated through the initial redox process, which renders it difficult for the oxidized/reduced PC to control the timing of the second redox process. From this standpoint, we reasoned that a reaction

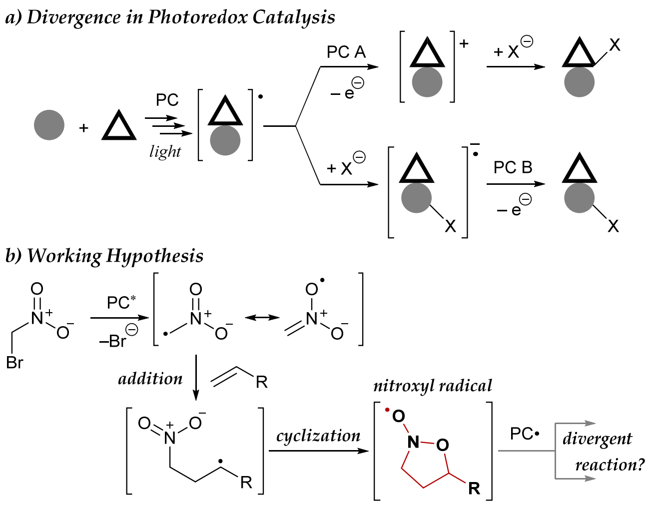

Fig. 1 (a) Schematic illustrations of divergent system in photoredox catalysis. (b) Working hypothesis for the formation of nitroxyl radical as a persistent junctional radical intermediate. PC = photocatalyst

---

Institute of Transformative Bio-Molecules (WPI-ITbM) and Department of Molecular and Macromolecular Chemistry, Graduate School of Engineering, Nagoya University, Nagoya 464-8601, Japan. Email: tooi@chembio.nagoya-u.ac.jp

†Electronic Supplementary Information (ESI) available: General experimental procedures, spectroscopic data for all new compounds, mechanistic investigations and computational details. See DOI: 10.1039/x0xx00000x

View Article Online
DOI: 10.1039/D0CC04821E

that involves the generation of a persistent radical as the junctional intermediate would provide a suitable platform for demonstrating the feasibility of controlling the reaction pathway by the use of a PC with pertinent redox potential. This consideration led us to select the reaction of α-bromo nitroalkanes with alkenes, expecting that the addition of the initially formed α-nitro alkyl radical to alkene followed by an intramolecular cyclization would generate a dihydroisoxazoline-*N*-oxyl as the persistent radical (Fig. 1b).[9]

An initial investigation was made by conducting the reaction of α-bromo nitroalkane **1a** ($E_{\mathrm{red}} = -0.87$ V vs. saturated calomel electrode (SCE))[10] with styrene (**2a**) in acetonitrile (MeCN) in the presence of 2,4,6-collidine as a base (1 equiv) and Ir(ppy)$_3$ as the representative PC (1 mol%) with an excited-state oxidation potential ($E^*_{\mathrm{ox}} = -1.97$ V vs. SCE)[11c] sufficient for the single-electron reduction of **1a** under irradiation of blue LEDs (456 nm). Smooth consumption of **1a** was observed after 5 h of stirring at ambient temperature, affording a mixture of two addition products, isoxazoline-*N*-oxide **3a** and γ-bromo nitroalkane **4a**, in a ratio of 40:18 (Table 1, entry 1). Subsequent evaluation of the effect of the PC properties revealed that the distribution of **3a** and **4a** was sensitive to the ground-state redox potential ($E_{1/2}$ (Ir$^{\mathrm{IV}}$/Ir$^{\mathrm{III}}$) vs. SCE). When less oxidizing Ir(tbppy)$_3$ was used, the preferential formation of **3a** was significantly enhanced (entry 2). Furthermore, **3a** was obtained almost exclusively by the addition of Ph$_3$N (1.0 equiv) ($E_{\mathrm{ox}} = +0.94$ V vs. SCE)[10] as a single-electron reductant under otherwise identical conditions (entry 3).

Table 1 Reaction optimization[a]

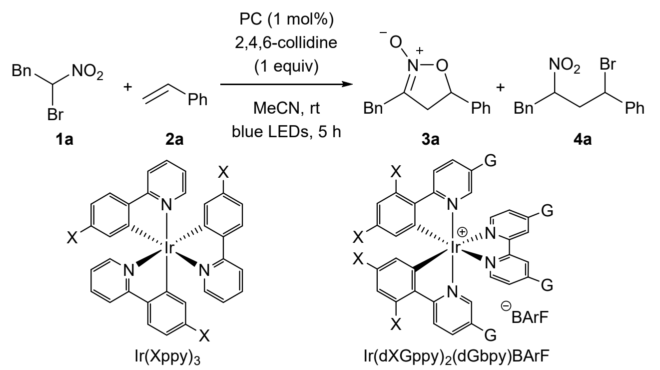

entry	PC/additive (1 equiv)	$E_{1/2}$ (Ir$^{\mathrm{IV}}$/Ir$^{\mathrm{III}}$) (V vs. SCE)	yield (**3a**)[b]	yield (**4a**)[b]
1	Ir(ppy)$_3$	+0.78[c]	40	18
2	Ir(tbppy)$_3$	+0.69[c]	59	11
3	Ir(tbppy)$_3$/Ph$_3$N[d]	—	54	<5
4	Ir(Fppy)$_3$	+1.00[c]	26	29
5	Ir(CF$_3$ppy)$_3$	+1.11[c]	17	35
6	Ir(ppy)$_2$(dtbbpy)BArF	+1.21[c]	<5	54
7	Ir(4Fppy)$_2$(dtbbpy)BArF	+1.49[c]	<5	44
8	Ir(dFCF$_3$ppy)$_2$(dCF$_3$bpy)BArF	+1.93[c]	<5	62
9	Ir(ppy)$_2$(dtbbpy)BArF/Ph$_3$N[d]	—	47	<5

[a] Reactions were conducted with 0.10 mmol of **1a** and 0.20 mmol of **2a** in the presence of 1 mol% of photocatalyst (PC) and 2,4,6-collidine (1 equiv) in MeCN at ambient temperature for 5 h under irradiation of blue LEDs (456 nm). [b] Determined by ^{1}H NMR (400 MHz) using trimethylsilylbenzene as an internal standard (average of two runs). **4a** was obtained as a diastereomeric mixture (ca. 1:1). [c] reference 11. [d] 1.0 equiv of Ph$_3$N was added. BArF = (3,5-(CF$_3$)$_2$C$_6$H$_3$)$_4$B$^-$

On the other hand, the increase in the oxidation ability of PC in the Ir$^{\mathrm{IV}}$ state pronounced the opposite preference as seen in the reactions with Ir(Fppy)$_3$ and Ir(CF$_3$ppy)$_3$ (entries 4 and 5). Moreover, employing cationic Ir complexes with even higher oxidation ability of the Ir$^{\mathrm{IV}}$ state (the oxidative condition) led to the exclusive formation of **4a**, regardless of the pyridyl ligand structures (entries 6~8). Interestingly, under the oxidative condition established with Ir(ppy)$_2$(dtbbpy)BArF as a PC, the Ph$_3$N additive totally reversed the product distribution to the predominant formation of **3a** (the reductive condition) (entry 9). This observation uncovered that the oxidative or reductive condition can be achieved using the same PC with the respective absence or presence of Ph$_3$N. The action of Ph$_3$N as a reductant would suppress the generation of an oxidative Ir$^{\mathrm{IV}}$ species, which appears to be crucial for the selective production of **3a**. In other words, an intermediate requisite for the formation of **4a** was only generated by a highly oxidizing Ir complex, indicating that efficient oxidation of the intermediary dihydroisoxazoline-*N*-oxyl radical is of significant importance.

We next carried out experiments to gain mechanistic insight. ^{1}H NMR monitoring of the reaction progress indicated that the product distribution was kinetically determined (Fig. 2). This was further supported by examining the possible interconversion between products **3a** and **4a** (eq. S1~3). Exposure of **3a** to the oxidative condition resulted in decomposition without the formation of **4a**. When **4a** was subjected to the reductive condition, most of it was consumed to give unidentified products with concurrent conversion to **3a** (30%). We also performed luminescence quenching (Stern-Volmer plot) experiments, which showed that both of photoexcited Ir(tbppy)$_3$ and Ir(ppy)$_2$(dtbbpy)BArF could be oxidatively quenched by **1a** but not by **2a** ($E_{\mathrm{red}} = -2.58$ V vs. SCE)[11a] (Fig. S9). It should be noted that **1a** and Ph$_3$N quenched photoexcited Ir(ppy)$_2$(dtbbpy)BArF at comparable rate, suggesting the intervention of an alternative, reductive quenching-initiated mechanism under the reductive condition.

Based on these observations and the overall reaction outcome, plausible mechanisms are depicted in Fig. 3. The initial single-electron reduction of **1** by the photoexcited Ir$^{\mathrm{III}}$ complex followed by mesolytic cleavage of the C-Br bond generates α-nitro alkyl radical and the oxidized Ir$^{\mathrm{IV}}$ complex in the form of a bromide salt. Subsequent addition of the alkyl radical species to

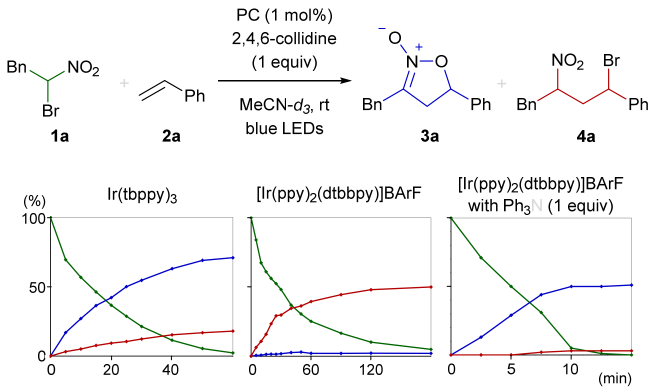

Fig. 2 Time course of the reaction (green: **1a**, blue: **3a**, and red: **4a**).

View Article Online
DOI: 10.1039/D0CC04821F

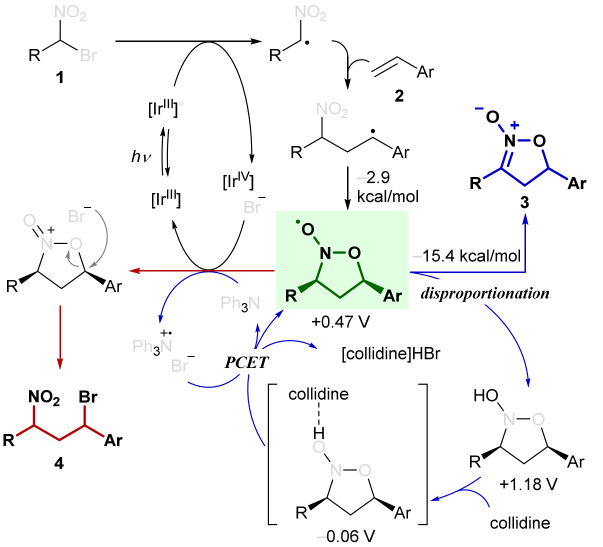

Fig. 3 Plausible reaction mechanisms under the oxidative (red arrows) and reductive (blue arrows) conditions with Ir(ppy)$_2$(dtbbpy)BArF as a photocatalyst. Indicated redox potentials (vs. SCE) and relative energy differences (Δ*G*) were estimated by DFT calculations for the process via thermodynamically more stable *syn*-isomer of the cyclic nitroxyl radical (R = Me, Ar = Ph) (SMD(MeCN)-(U)B3LYP/6-31+G(d,p)-LanL2DZ//SMD(MeCN)-(U)B3LYP/6-31G(d)-LanL2DZ level).

2 affords a β-nitro benzylic radical that undergoes spontaneous cyclization to furnish the dihydroisoxazoline-*N*-oxyl (nitroxyl) radical as a key persistent radical intermediate. The susceptibility of the transient β-nitro benzylic radical toward cyclization is ascribable to the known radicophilicity of the nitro moiety.[9,12] The energy profile was estimated by density functional theory (DFT) calculations (SMD(MeCN)-(U)B3LYP/6-31+G(d,p)-LanL2DZ//SMD(MeCN)-(U)B3LYP/6-31G(d)-LanL2DZ level) with the nitroxyl radical possessing methyl (R) and phenyl (Ar) groups revealed that this intramolecular process is exothermic (Δ*G* = –2.9 kcal·mol^{-1}).[13]

The nitroxyl radical then serves as a junctional intermediate as the following reaction diverges depending on the PC and reaction conditions. When the Ir^{IV} complex has a high oxidation ability,[14] it abstracts an electron from the nitroxyl radical to generate the five-membered *N*-oxo-dihydroisoxazolinium (nitroxonium) ion and the pairing bromide ion spontaneously engages in a pseudo-intramolecular ring-opening reaction to produce **4** (the oxidative condition, red arrows). On the other hand, under the reductive condition, Ph_3N rapidly quenches the Ir^{IV} complex and the elimination of the strong oxidant allows highly exothermic disproportionation of the nitroxyl radical to form **3** (Δ*G* = –15.4 kcal·mol^{-1}) (blue arrows). This process concomitantly generates *N*-hydroxyl dihydroisoxazoline, and its oxidation potential (E_{ox} = +1.18 V vs. SCE) is significantly higher than that of Ph_3N.[16] Yet, it is likely restored to the junctional intermediate via a proton-coupled electron transfer (PCET)[17] under the influence of 2,4,6-collidine, which was expected from the considerable difference in the oxidation potentials of the hydrogen-bonding complex (E_{ox} = –0.06 V vs. SCE) and the parent *N*-hydroxyl dihydroisoxazoline. It is relevant to add that the way of participation of Ph_3N in the redox processes is the same when a highly reducing PC such as Ir(tbppy)$_3$ is employed. However, the corresponding Ir^{IV} complex with low oxidation ability would exert intrinsic selectivity toward oxidizing the *N*-hydroxyl dihydroisoxazoline intermediate with the aid of 2,4,6-collidine, rather than oxidizing the nitroxyl radical (Fig. S18a). Meanwhile, we recognized that the intervention of a reductive quenching-initiated alternative mechanism should also be considered under the reductive condition (Fig. S19b). After the single-electron reduction of the photoexcited Ir^{III} complex by Ph_3N, swift transfer of an electron from the resulting Ir^{II} complex to **1** gave the radical anion of **1**, thus initiating the reaction sequence to reach the nitroxyl radical. Since the generation of the Ir^{IV}

Table 2 Substrate Scope[a]

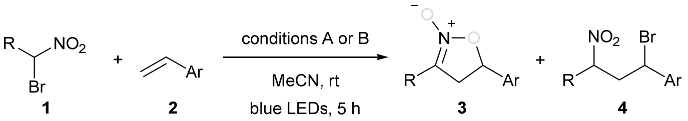

entry	R (**1**)	Ar (**2**)	Condition A[a]		Condition B[a]	
			yield[b]	**3**:**4**[c]	yield[b]	**3**:**4**[c]
1	Bn (**1a**)	2-MeC$_6$H$_4$ (**2b**)	54 (**3b**)	>20:1	50 (**4b**)	1:>20
2	**1a**	3-MeC$_6$H$_4$ (**2c**)	56 (**3c**)	>20:1	54 (**4c**)	1:>20
3	**1a**	4-MeC$_6$H$_4$ (**2d**)	55 (**3d**)	>20:1	59 (**4d**)	1:>20
4	**1a**	4-FC$_6$H$_4$ (**2e**)	60 (**3e**)	>20:1	45 (**4e**)	1:>20
5	**1a**	2-ClC$_6$H$_4$ (**2f**)	31 (**3f**)	>20:1	47 (**4f**)	1:>20
6	**1a**	3-ClC$_6$H$_4$ (**2g**)	30 (**3g**)	>20:1	53 (**4g**)	1:>20
7	**1a**	4-ClC$_6$H$_4$ (**2h**)	46 (**3h**)	>20:1	62 (**4h**)	1:>20
8	**1a**	4-^{t}BuC$_6$H$_4$ (**2i**)	57 (**3i**)	>20:1	58 (**4i**)	1:>20
9	**1a**	4-ClCH$_2$C$_6$H$_4$ (**2j**)	44 (**3j**)	>20:1	42 (**4j**)	1:>20
10	**1a**	4-AcOCH$_2$C$_6$H$_4$ (**2k**)	40 (**3k**)	>20:1	50 (**4k**)	1:>20
11	**1a**	4-Me$_3$SiCCC$_6$H$_4$ (**2l**)	48 (**3l**)	>20:1	40 (**4l**)	1:>20
12	Me (**1b**)	Ph (**2a**)	59 (**3m**)	>20:1	41 (**4m**)	1:>20
13	Et (**1c**)	**2a**	51 (**3n**)	>20:1	64 (**4n**)	1:>20
14	Me(CH$_2$)$_8$ (**1d**)	**2a**	51 (**3o**)	>20:1	42 (**4o**)	1:>20

[a] Reactions were performed with 0.10 mmol of **1**, 0.20 mmol of **2**, and 0.10 mmol of 2,4,6-collidine in MeCN at ambient temperature for 5 h under irradiation of blue LEDs (456 nm); condition **A**: 1 mol% of Ir(ppy)$_2$(dtbbpy)BArF and 0.10 mmol of Ph_3N; condition **B**: 1 mol% of Ir(ppy)$_2$(dtbbpy)BArF. [b] Isolated yield is indicated. **4** was obtained as a diastereomeric mixture (ca. 1:1). [c] Product ratio was determined by ^{1}H NMR (400 MHz).

View Article Online
DOI: 10.1039/D0CC04821F

complex with high oxidation ability is not involved, single-electron oxidation of the junctional intermediate does not occur, preventing the formation of **4**.

The scope of the present divergent photocatalytic system was explored with various styrenes **2** and α-bromo nitroalkanes **1** (Table 2). Although the chemical yield was generally moderate, virtually complete control of the reaction pathway was consistently realized irrespective of the electronic and steric features of **2** (entries 1~11). A similarly strict divergence was also feasible in reactions with other α-bromo nitroalkanes **1** bearing linear aliphatic substituents (entries 12~14).

In conclusion, we have established a divergent photocatalytic system for the reaction of α-bromo nitroalkanes with styrene derivatives under visible-light irradiation. The generation of the persistent nitroxyl radical as a junctional intermediate and proper tuning of the redox ability of the Ir-based photocatalysts constitute the crucial elements for achieving the regorous control over the reaction pathways to produce two distinct products with sufficient structural diversity. This study showcases the possibility of developing catalyst-directed divergent reactions by taking advantage of the intrinsic nature of photoredox catalysis and stimulates further research endeavors to explore the synthetic potential of redox-regulated, divergent radical transformations.

Financial support was provided by CREST-JST (JPMJCR13L2: 13418441, to TO), a Grant-in-Aid for Scientific Research on Innovative Areas “Hybrid Catalysis” (No. 17H06444, to TO), and "Graduate Program of Transformative Chem-Bio Research" in Nagoya University, supported by MEXT (WISE Program), and Grants of JSPS for Scientific Research. YT acknowledges JSPS for financial support.

Conflicts of interest

There are no conflicts to declare.

Notes and references

1 (a) J. Mahatthananchai, A. M. Dumas and J. W. Bode, *Angew. Chem. Int. Ed.*, 2012, **51**, 10954. (b) S. Krautwald and E. M. Carreira, *J. Am. Chem. Soc.*, 2017, **139**, 5627.

2 (*a*) V. Kottisch, Q. Michaudel and B. P. Fors, *J. Am. Chem. Soc.*, 2017, **139**, 10665; (*b*) J. Li, Y. Luo, H. W. Cheo, Y. Lan and J. Wu, *Chem*, 2019, **5**, 192.

3 (*a*) A. Singh, C. J. Fennell and J. D. Weaver, *Chem. Sci.*, 2016, **7**, 6796; (*b*) M. J. James, J. L. Schwarz, F. Strieth-Kalthoff, B. Wibbeling and F. Glorius, *J. Am. Chem. Soc.*, 2018, **140**, 8624.

4 (*a*) D. B. Bagal, G. Kachkovskyi, M. Knorn, T. Rawner, B. M. Bhanage and O. Reiser, *Angew. Chem. Int. Ed.*, 2015, **54**, 6999; (*b*) H. Wang, Y. Man, Y. Xiang, K. Wang, N. Li and B. Tang, *Chem. Commun.*, 2019, **55**, 11426; (*c*) Y. Gao, Y. Liu and J.-P. Wan, *J. Org. Chem.*, 2019, **84**, 2243.

5 (*a*) J. Du, L. R. Espelt, I. A. Guzei and T. P. Yoon, *Chem. Sci.*, 2011, **2**, 2115; (*b*) S. Zhu, A. Das, L. Bui, H. Zhou, D. P. Curran and M. Rueping, *J. Am. Chem. Soc.*, 2013, **135**, 1823; (*c*) C. Zhang, S. Li, F. Bureš, R. Lee, X. Ye and Z. Jiang, *ACS Catal.*, 2016, **6**, 6853; (*d*) M. Mei, D. Anand and L. Zhou, *Org. Lett.*, 2019, **21**, 3548.

6 For representative examples, see; (*a*) H. Jiang, Y. Cheng, Y. Zhang and S. Yu, *Org. Lett.*, 2013, **15**, 4884; (*b*) Y. Liu, R.-J. Song, S. Luo and J.-H. Li, *Org. Lett.*, 2018, **20**, 212; (*c*) J. Hou, A. Ee, W. Feng, J.-H. Xu, Y. Zhao and J. Wu, *J. Am. Chem. Soc.*, 2018, **140**, 5257; (*d*) H. Liang, G.-Q. Xu, Z.-T. Feng, Z.-Y. Wang and P.-F. Xu, *J. Org. Chem.*, 2019, **84**, 60; (*e*) Z.-S. Wang, Y.-B. Chen, H.-W. Zhang, Z. Sun, C. Zhu and L.-W. Ye, *J. Am. Chem. Soc.*, 2020, **142**, 3636; (*f*) J. Ma, F. Schäfers, C. Daniliuc, K. Bergander, C. A. Strassert and F. Glorius, *Angew. Chem. Int. Ed.*, 2020, **59**, 9639.

7 J. Cheng, Y. Cheng, J. Xie and C. Zhu, *Org. Lett.*, 2017, **19**, 6452.

8 (*a*) X.-J. Wei, W. Boon, V. Hessel and T. Noël, *ACS Catal.*, 2017, **7**, 7136; (*b*) S. K. Pagire, A. Hossain and O. Reiser, *Org. Lett.*, 2018, **20**, 648; (*c*) J.-h. Xu, W.-b. Wu and J. Wu, *Org. Lett.*, 2019, **21**, 5321; (*d*) C. Kerzig and O. S. Wenger, *Chem. Sci.*, 2019, **10**, 11023.

9 (*a*) W. R. Bowman, D. S. Brown, C. A. Burns and D. Crosby, *J. Chem. Soc. Perkin Trans. 1*, 1993, 2099; (*b*) R. Warsinsky and E. Steckhan, *J. Chem. Soc. Perkin Trans. 1*, 1994, 2027; (*c*) A.-C. Durand, E. Dumez, J. Rodriguez and J.-P. Dulcère, *Chem. Commun.*, 1999, 2437; (*d*) B. B. Snider and Q. Che, *Tetrahedron*, 2002, **58**, 7821.

10 See ESI for determination of the redox potential.

11 (*a*) G. Filardo, S. Gambino, G. Silvestri, A. Gennaro and E. Vianello, *J. Electroanal. Chem. Interfacial Electrochem.*, 1984, **177**, 303; (*b*) M. S. Lowry, J. I. Goldsmith, J. D. Slinker, R. Rohl, R. A. Pascal, Jr., G. G. Malliaras and S. Bernhard, *Chem. Mater.*, 2005, **17**, 5712; (*c*) A. Singh, K. Teegardin, M. Kelly, K. S. Prasad, S. Krishnan and J. D. Weaver, *J. Organomet. Chem.*, 2015, **776**, 51; (*d*) G. J. Choi, Q. Zhu, D. C. Miller, C. J. Gu and R. R. Knowles, *Nature*, 2016, **539**, 268.

12 J. Davies, S. G. Booth, S. Essafi, R. A. W. Dryfe and D. Leonori, *Angew. Chem. Int. Ed.*, 2015, **54**, 14017.

13 The indicated energy was calculated for the thermodynamically favorable, *syn*-diastereomer. The full potential energy diagram including the transition sate energies is depicted in ESI.

14 Although the experimentally determined reduction potential of Ir(ppy)$_2$(dtbbpy)$^{2+}$ was reported to be +1.21 V vs. SCE,[11b] the value calculated by following the literature method[14] (+0.93 V) was considered for the discussion based on the comparison with the calculated potentials of the intermediates.

15 H. G. Roth, N. A. Romero and D. A. Nicewicz, *Synlett*, 2016, **27**, 714.

16 The calculated[14] oxidation potential of Ph$_3$N (+0.56 V) was considered for the discussion instead of the experimentally determined value (+0.94 V vs. SCE).[10]

17 D. R. Weinberg, C. J. Gagliardi, J. F. Hull, C. F. Murphy, C. A. Kent, B. C. Westlake, A. Paul, D. H. Ess, D. G. McCafferty, and T. J. Meyer, *Chem. Rev.* **2012**, *112*, 4016.

View Article Online
DOI: 10.1039/D0CC04821F

Table of Contents Entry

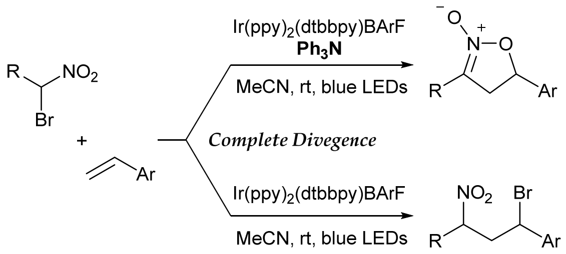

A divergent photocatalytic system for the reaction of α-bromo nitroalkanes with styrene derivatives is established.